

The isovector/isoscalar ratio of the imaginary part of the intermediate-energy nucleon optical model potential studied by the quantum molecular dynamics

Satoshi Chiba, Koji Niita, Tokio Fukahori, Tomoyuki Maruyama,
Toshiki Maruyama and Akira Iwamoto
*Japan Atomic Energy Research Institute,
Tokai-mura, Naka-gun, Ibaraki-ken 319-11, Japan*

Abstract

Energy dependence of the ratio of the isovector and isoscalar strengths in the imaginary part of the nucleon optical model potential at the medium energy range was extracted from an analysis of proton and neutron induced total reaction cross sections on ^{11}Li with a theoretical framework called quantum molecular dynamics (QMD). The isovector/isoscalar ratio was found to be about 0.8 at 100 MeV, and decreased almost linearly in $\log(E)$ to 0 at several hundred MeV. This result was consistent with an estimate at lower energy, and was also in good accord with the values used by Kozack and Madland for the analysis of nucleon + ^{208}Pb reactions.

I. INTRODUCTION

In recent years, the intermediate-energy nuclear reactions have come to be more and more important for various reasons related with not only the basic but also the applied research fields [1]. It is obvious that the optical model potential (OMP) remains to be an important quantity in the researches of nucleon-induced nuclear reactions at medium energy range as was the case at the lower energy region.

The nucleon optical potential has been studied intensively in the past by many authors from many points of view [2–19]. It is known that the proposed potentials give excellent results in many cases. However, it is also recognized that they are still far from perfect in many aspects, and there are many ambiguities which prevent the OMP to be defined uniquely. If we look into the status of the imaginary isovector part of the OMP, the situation seems to be particularly poor: In the low energy region where the surface absorption is dominant, the strength of the surface imaginary isovector potential is distributed in the range from 9 MeV [10] to 16 MeV [9]. This shows that the imaginary isovector strength has an ambiguity as large as a factor of 2 in spite of the huge efforts to define the potential at low energy region where both the neutron and proton data are available. At the intermediate energy region where the volume absorption becomes dominant, the proposed global potentials do not give the isovector volume imaginary potential explicitly [3–12] (except one by Kozack and Madland [13]). This is against the idea of the Lane model [20] (and its relativistic extension [21]) on which the OMPs have been based. It is true that the difference of the nucleon-nucleon (N-N) interaction between the identical (p-p, or n-n) and non-identical (p-n) pairs

of nucleons, that is the origin of the isovector term in OMP, becomes smaller and smaller as energy increases, and finally reaches to zero at several hundred MeV. This fact, together with small asymmetry $((N - Z)/A)$ range spanned by most of the stable nuclei, may make the net effect of the isovector part less and less significant in the intermediate-energy region. However, it cannot be a justification of ignoring the imaginary isovector term from the basic point of view.

For exotic nuclei such as ^{11}Li , the effects of imaginary isovector term will be significant because they have large asymmetry parameters. In the case of ^{11}Li , there are 8 neutrons and only 3 protons. Due to the big difference between the proton and neutron numbers, the isovector effects will be magnified in these nuclei. Furthermore, these exotic nuclei are known to have an outer region consisting only of neutrons, i.e., the neutron halo or neutron skin [22]. Due to this structure, the incident particles will interact firstly with only neutrons, so it is expected for these nuclei to respond quite differently depending on the (z -component of the) projectile isospin. Therefore the effects of the isospin-dependent N-N interaction will still be noticeable for such exotic nuclei at intermediate energy while the Coulomb correction is kept to be negligible.

It is the basic idea of this work to use the feature of the exotic nuclei as an amplifier of the isospin-dependence in the N-N interaction to investigate the imaginary isovector OMP. For this aim ^{11}Li was selected as the target nucleus, and the total reaction cross sections for neutron and proton projectiles were calculated by a theoretical framework called quantum molecular dynamics (QMD) [23–25]. We use a QMD framework developed at JAERI [26], which has been used intensively for investigations of light-ion induced reaction mechanisms at intermediate energy region [27–30]. This framework, however, was not satisfactory in several senses. We then modified it for the present purpose as 1) to be Lorentz covariant [31], 2) to include the momentum dependence in the effective N-N interaction, 3) to include the Pauli potential to simulate the Fermion nature of the nucleon system better, and 4) to include a revised N-N collision term. As a check of the new framework, we have carried out an analysis of total reaction cross sections for carbon target with various kinds of projectiles, including ^{11}Li , for which experimental data are available.

II. BRIEF EXPLANATION OF THE QMD

The details of the formulation we adopted will be given elsewhere [32], so only a simple explanation is given in this paper. We start from representing each nucleon (denoted by a subscript i) by a Gaussian wave packet in both the coordinate and momentum spaces. The total wave function is assumed to be a direct product of these wave functions. Thus the one-body distribution function is obtained by the Wigner transform of the wave function,

$$f(\mathbf{r}, \mathbf{p}) = \sum_i f_i(\mathbf{r}, \mathbf{p}) = \sum_i 8 \cdot \exp \left[-\frac{(\mathbf{r} - \mathbf{R}_i)^2}{2L} - \frac{2L(\mathbf{p} - \mathbf{P}_i)^2}{\hbar^2} \right] \quad (1)$$

where L is a parameter which represents the spacial spread of a wave packet, \mathbf{R}_i and \mathbf{P}_i corresponding to the centers of a wave packet in the coordinate and momentum spaces, respectively. The equation of motion of \mathbf{R}_i and \mathbf{P}_i is given, on the basis of the time-dependent variational principle, by the Newtonian equation:

$$\dot{\mathbf{R}}_i = \frac{\partial H}{\partial \mathbf{P}_i}, \quad \dot{\mathbf{P}}_i = -\frac{\partial H}{\partial \mathbf{R}_i}, \quad (2)$$

and the stochastic N-N collision term [26,36]. The Hamiltonian H was taken to be a sum of the zero-th component of the 4-momentum vector of each particle [31]:

$$H = \sum_i p_i^0 = \sum_i \sqrt{\mathbf{P}_i^2 + m_i^2 + 2m_i U_i} \quad (3)$$

The scalar potential U_i consists of the Skyrme-type effective N-N interaction [35], Coulomb and symmetry energy terms, the Pauli potential and the momentum-dependent potentials:

$$\begin{aligned} U_i = & \frac{1}{2} \frac{A}{\rho_0} \langle \rho_i \rangle + \frac{1}{1 + \tau} \frac{B}{\rho_0^\tau} \langle \rho_i \rangle^\tau + \frac{1}{2} \sum_{j(\neq i)} c_i c_j \frac{e^2}{\Delta \tilde{q}_{ij}} \operatorname{erf} \left(\Delta \tilde{q}_{ij} / \sqrt{4L} \right) \\ & + \frac{C_s}{2\rho_0} \sum_{j(\neq i)} (1 - 2|c_i - c_j|) \rho_{ij} + \sum_{j(\neq i)} V_{Pauli_{ij}} \\ & + \frac{V_{ex}^{(1)}}{2\rho_0} \sum_{j(\neq i)} \frac{1}{1 + [\Delta \tilde{p}_{ij} / \mu_1]^2} \rho_{ij} + \frac{V_{ex}^{(2)}}{2\rho_0} \sum_{j(\neq i)} \frac{1}{1 + [\Delta \tilde{p}_{ij} / \mu_2]^2} \rho_{ij} \end{aligned} \quad (4)$$

where "erf" denotes the error function, and c_i is 1 for proton, and 0 for neutron. Other symbols in this equation are defined as

$$\begin{aligned} \langle \rho_i \rangle &= \sum_{j \neq i} \rho_{ij} = \sum_{j \neq i} \int d\mathbf{r} \rho_i(\mathbf{r}) \rho_j(\mathbf{r}) \\ &= \sum_{j \neq i} (4\pi L)^{-3/2} \exp \left[-\Delta \tilde{q}_{ij}^2 / 4L \right] \\ \rho_i &= \int \frac{d\mathbf{p}}{(2\pi\hbar)^3} f_i(\mathbf{r}, \mathbf{p}) \\ V_{Pauli_{ij}} &= \frac{1}{2} V_P \left[\frac{\hbar}{q_0 p_0} \right]^3 \exp \left[-\frac{\Delta \tilde{q}_{ij}^2}{2q_0^2} - \frac{\Delta \tilde{p}_{ij}^2}{2p_0^2} \right] \delta_{\tau_i \tau_j} \delta_{\sigma_i \sigma_j} \\ \Delta \tilde{q}_{ij}^2 &= -\Delta q_{ij}^2 + \frac{(\Delta q_{ij} p_{ij})^2}{p_{ij}} \\ \Delta \tilde{p}_{ij}^2 &= -\Delta p_{ij}^2 + \frac{(\Delta p_{ij} p_{ij})^2}{p_{ij}} \end{aligned} \quad (5)$$

and

$$\begin{aligned} \Delta q_{ij} &= q_i - q_j \\ \Delta p_{ij} &= p_i - p_j \\ p_{ij} &= p_i + p_j \end{aligned} \quad (6)$$

The q_i and p_i are the coordinate and momentum of particle i in the 4-vector representation, respectively. It is easy to note that the variables $\Delta \tilde{q}_{ij}^2$ and $\Delta \tilde{p}_{ij}^2$ defined above are Lorentz scalars. In addition, this form of Hamiltonian gives the equation-of-motion equivalent with the Relativistic QMD [33,34] with a special choice of the time-fixation [31].

The parameters in the above Hamiltonian were determined to reproduce the saturation density $\rho = \rho_0 = 0.168 \text{ fm}^{-3}$, minimum energy $E/A = -16 \text{ MeV}$, the energy dependence of the real optical model potential, and the effective mass $m^*/m = 0.8$ at the Fermi surface. Furthermore, the parameters of the Pauli potential were chosen for the kinetic energy of the QMD to be equal to the total energy of the free Fermion systems [24]. From these conditions, the following values were determined: $A = -127.68 \text{ MeV}$, $B = 204.28 \text{ MeV}$, $\tau = 4/3$, $C_s = 25 \text{ MeV}$, $V_{ex}^{(1)} = -258.54 \text{ MeV}$, $V_{ex}^{(2)} = -375.60 \text{ MeV}$, $\mu_1 = 2.35 \text{ MeV}$, $\mu_2 = 0.4 \text{ MeV}$, $L = 1.75 \text{ fm}^2$, $V_p = 140.0 \text{ MeV}$, $p_0 = 120.0 \text{ MeV}$, and $q_0 = 1.644 \text{ fm}$.

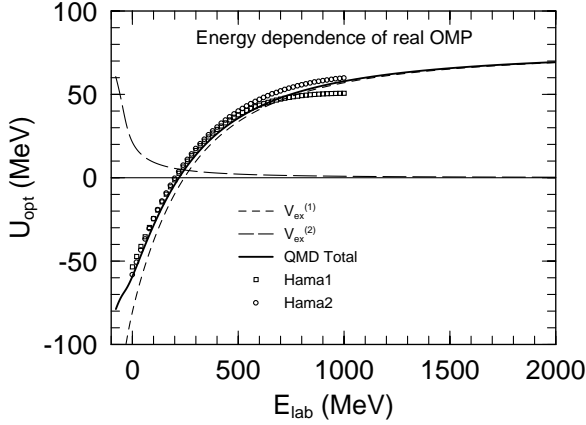


Fig. 1 Energy dependence of the real part of OMP

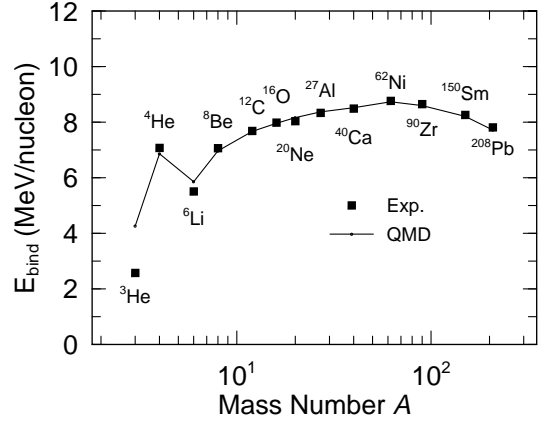


Fig. 2 Binding energy per nucleon

Fig. 1 shows the energy dependence of the real part of the OMP. The solid curve shows the potential depth calculated from Eq. (4) without the Coulomb and the Pauli potentials. It is understood that the present parameterization reproduces the energy dependence of real OMP obtained experimentally [12] fairly well. The binding energies per nucleon of several stable nuclei calculated with QMD are compared with experimental data in Fig. 2. This figure shows that the QMD calculation gives a very good description of such basic nuclear structure information.

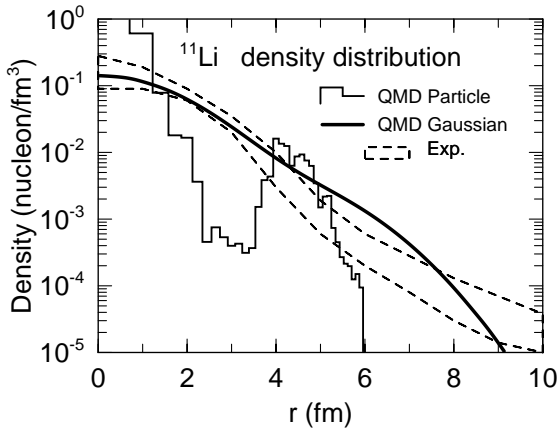


Fig. 3 Nucleon density distribution of ^{11}Li

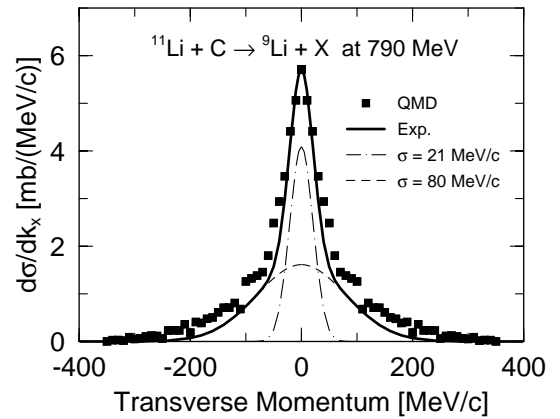


Fig. 4 Transverse momentum distribution of ^9Li from the $^{11}\text{Li} + \text{C}$ reaction at 790 MeV/A

The nucleon density distribution of ^{11}Li is shown in Fig. 3 with the experimental data [22]. The smooth curve denotes the nucleon distribution calculated by QMD while the broken curves denote the upper and lower bounds of the experimental uncertainty [22]. In the same

figure, we show the "particle" distribution by the histogram, which means the distribution of the center of the Gaussian wave packets. The "particle" distribution shows the existence of valence neutrons outside a core (${}^9\text{Li}$). The neutron halo structure is reproduced well by the present calculation. The binding energy for ${}^{11}\text{Li}$ was calculated to be 44.89 MeV, which is consistent with the experimental value of 45.54 MeV. Fig. 4 shows the transverse momentum of ${}^9\text{Li}$ for the reaction ${}^{11}\text{Li} + \text{C}$ at 790 MeV per nucleon. The 2 components in the experimental data by Tanihata et al. [22] are reproduced excellently by the QMD calculation.

III. CALCULATION OF REACTION CROSS SECTIONS FOR ${}^{12}\text{C}$ TARGET AS A VERIFICATION OF THE COMPUTATIONAL METHOD

The reaction cross section was calculated based on the following formula, which is equivalent with the optical limit of the Glauber approximation:

$$\sigma_R = 2\pi \int b(1 - T(b))db \quad (7)$$

where the $T(b)$ denotes the transparency, i.e., the probability that the projectile having the impact parameter b causes no interaction with the target nucleons. In the Glauber approximation, such quantity is evaluated along a straight line trajectory, while in QMD it is calculated on a more realistic trajectory determined by the mean-field described by the effective two-body potential Eq.(4) including the Coulomb interaction.

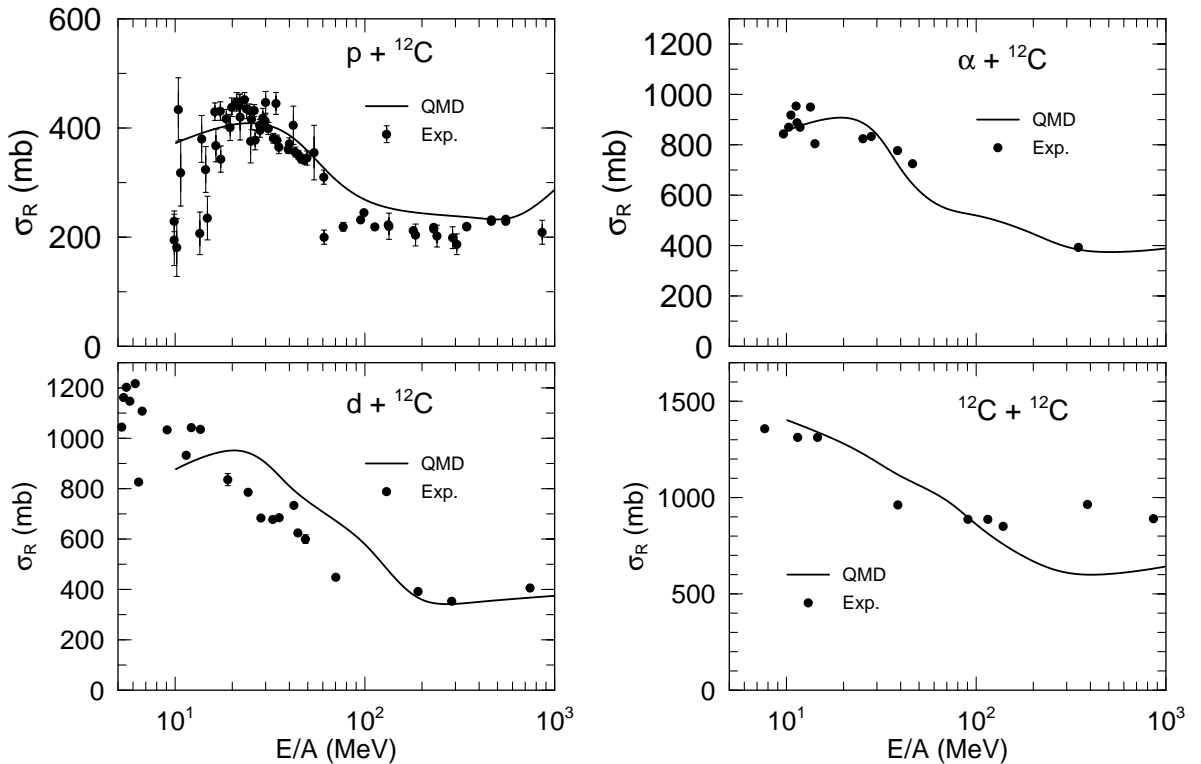


Fig. 5 Total reaction cross sections of ${}^{12}\text{C}$ for incident proton (left-top), deuteron (left-bottom), α (right-top) and ${}^{12}\text{C}$ (right-bottom).

The reaction cross sections for ^{12}C were calculated for projectiles of proton, deuteron, α and ^{12}C , and are shown in Fig. 5 with experimental data [37–40]. These figures confirm that the QMD gives satisfactory descriptions of the reaction cross sections of various projectiles on carbon even though no parameter was adjusted for this purpose. The only exception is the case of $d + ^{12}\text{C}$ for which the QMD overestimates the reaction cross section noticeably. The reason of this was found to be related with the stability of deuterium in the QMD simulation: Deuterium is a nuclei in which a proton and neutron bind each other with the binding energy of 1 MeV per nucleon. Such system is not stable enough in QMD calculation, so it breaks into a neutron and proton when it reaches to the carbon target and feels the mean-field (real OMP) of the target without causing any N-N collision (which is the origin of the imaginary OMP). In other cases, it could be concluded that the QMD calculation to be reliable.

The total reaction cross sections for ^{12}C target induced by several Li isotopes are shown in Fig. 6. Again, the QMD calculation reproduces the basic feature of the experimental data [41,42]. The agreement is particularly good for ^{11}Li on ^{12}C case.

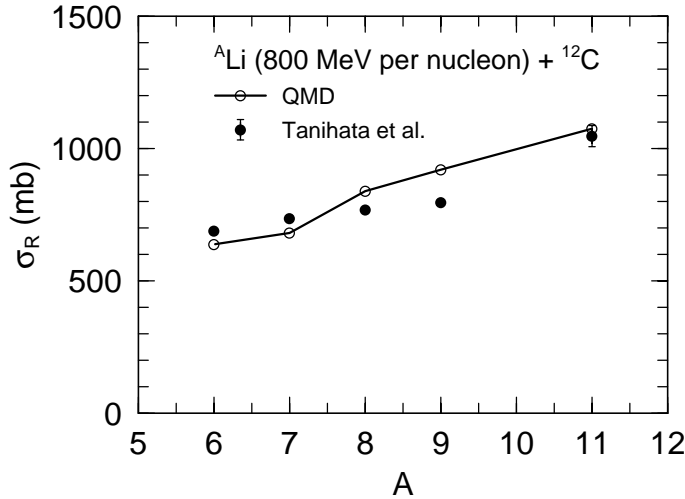


Fig. 6 Total reaction cross sections of ^{12}C for incident ^ALi , where $A = 6, 7, 8, 9$ and 11 .

IV. EXTRACTION OF THE ISOVECTOR/ISOSCALAR RATIO OF IMAGINARY NUCLEON OMP AT INTERMEDIATE ENERGY

Based on the success of the previous section, we proceed to extraction of the isovector/isoscalar ratio of the imaginary OMP. Firstly we define a quantity α to be

$$\alpha \equiv \frac{\sigma_R(p) - \sigma_R(n)}{\sigma_R(p) + \sigma_R(n)} \quad (8)$$

where $\sigma_R(i)$ denotes the total reaction cross section for incident particle i . The quantity α was calculated at 100, 200, 400 and 800 MeV for ^{11}Li target by QMD, and is shown in Fig. 7. This quantity is found to be about 0.27 at 100 MeV, so the isospin dependence in the N-N collision really affects the total proton and neutron cross sections significantly. Such difference, however, becomes smaller and smaller as energy increases, and the effect is negligible at several hundred MeV. This is an intuitively understandable behavior.

Then, we take the 1st order expansion of σ_R with respect to the imaginary OMP (W) around W_0 :

$$\sigma_R(W = W_0 \pm \epsilon W_1) = \sigma_R(W_0) \pm \epsilon W_1 \frac{\partial}{\partial W} \sigma_R(W_0) \quad (9)$$

where $+$ applies to incident protons and $-$ to neutrons, W_0 denotes the imaginary isoscalar strength, the W_1 the isovector strength, and $\epsilon \equiv (N - Z)/A$. By using this formula, the quantity α can be written also to be

$$\alpha = \frac{\epsilon W_1 \frac{\partial}{\partial W} \sigma_R(W_0)}{\sigma_R(W_0)} \quad (10)$$

The ratio W_1/W_0 is calculated by putting the 2 α 's in Eqs. (8) and (10) equal;

$$\frac{W_1}{W_0} = \frac{\sigma_R(p) - \sigma_R(n)}{\sigma_R(p) + \sigma_R(n)} \frac{\sigma_R(W_0)}{\frac{\partial}{\partial W} \sigma_R(W_0)} \frac{1}{\epsilon W_0} \quad (11)$$

The first factor of the right hand side was already obtained by the QMD calculation (Fig. 7). We have then calculated the 2nd factor by employing the following classical expression for σ_R obtained with the Glauber approximation for uniform sphere of radius R [43,44],

$$\sigma_R(W) = \pi R^2 \left(1 - 2 \frac{1 - (1 + 2RkW/E)e^{-2RkW/E}}{(2RkW/E)^2} \right) \quad (12)$$

where k denotes the wave number and E the projectile energy. The imaginary isoscalar strength W_0 was taken from Finlay's parameterization [45],

$$W_0 = 6.6 + \frac{15.353(E - 80)^2}{(E - 80)^2 + 137.8^2} \quad (13)$$

The ratio W_1/W_0 calculated based on Eq. (11) is shown in the left part of Fig. 8. This figure shows that the ratio W_1/W_0 has a value of about 0.8 at 100 MeV, then decreases almost linearly in $\log(E)$, and reaches to 0 at several hundred MeV. This energy dependence is consistent with that of the difference of the cross sections between the identical and non-identical pairs of nucleons. The error bar was obtained from the statistical uncertainty in the factor α , and by assuming (rather extremely) the error of W_0 to be 50 %. The main source of error comes from the uncertainty in W_0 at 100 MeV, while the statistical error is dominant at 800 MeV. Anyway, the results are rather insensitive to the choice of the W_0 parameter.

In the right part of Fig. 8, the low-energy limit of this ratio was calculated with the Walter-Guss potential [8] at 10 MeV, and plotted with the presently obtained results. The energy dependence obtained in this work extrapolates smoothly to the lower energy value. The result calculated from the parameters of Kozack and Madland [13] are shown by the dash-dotted curve in the same figure. These values were obtained by adding the (Lorentz) scalar and vector imaginary potential strengths for each of the isoscalar and isovector components. Their value is slightly higher than the present estimate at 100 MeV. However, these 2 curves become closer as energy increase, and finally they are consistent at 300 to 400 MeV region.

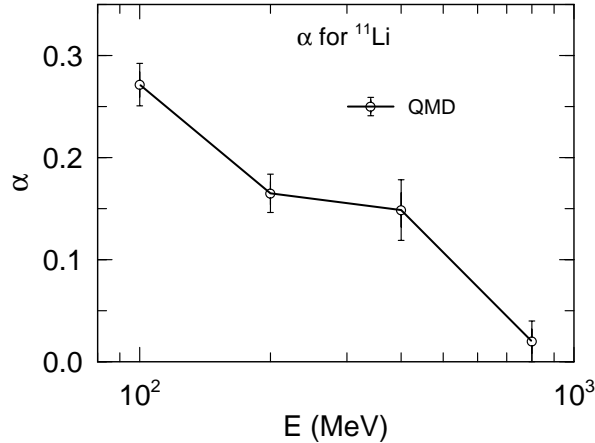


Fig. 7 The quantity α (defined in Eq. (8)) calculated by QMD for ^{11}Li

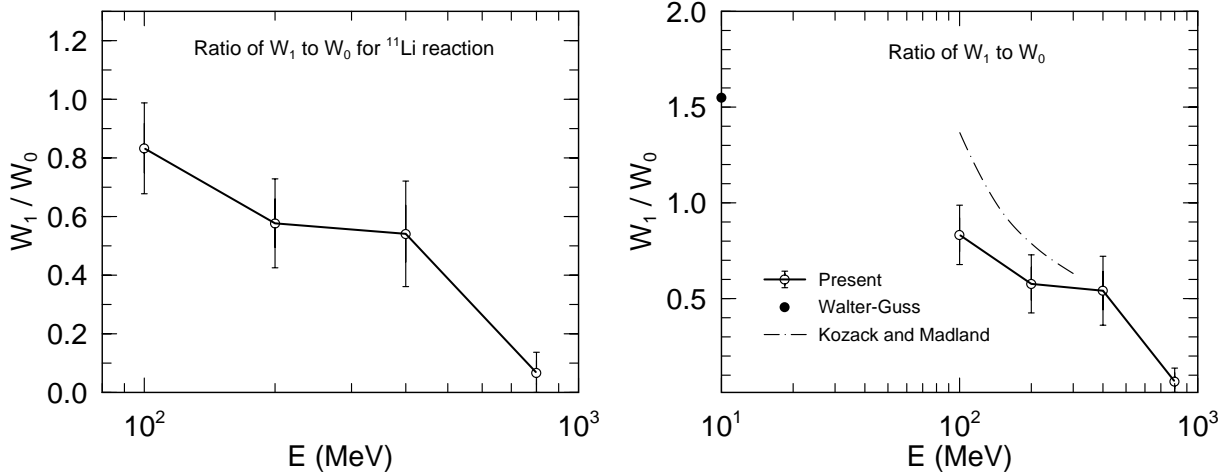


Fig. 8 The isovector / isoscalar ratio for imaginary nucleon OMP derived as Eq. (11). The left figure shows present result, while the right one includes the lower-energy estimate [8] and values used by Kozack and Madland [13].

V. CONCLUDING REMARKS

A QMD (quantum molecular dynamics) framework was used to extract information on the imaginary isovector term in the intermediate-energy nucleon OMP. The ^{11}Li was selected as an amplifier of the isospin-dependence in the nucleon-nucleon interaction which is the origin of the isovector potential. The difference in the reaction cross sections induced by neutron and proton on ^{11}Li indicated that the imaginary isovector potential plays a noticeable effect on the observables for such exotic nuclei at intermediate energy. The present result were found to be consistent with a lower energy estimate and with the values used by Kozack and Madland for the analysis of $N + ^{208}\text{Pb}$ observables.

The results of the present work are still preliminary and to be revised in future works.

REFERENCES

- [1] e.g., H. Yasuda, T. Tone and M. Mizumoto (Ed.), *The First Workshop of Neutron Science Research Program*, JAERI-conf 96-014(1996).
- [2] e.g., P.E. Hodgson, *The Nucleon Optical Model*, World Scientific (1994).
- [3] R.L. Varner, W.J. Thompson, T.L. McAbee, E.J. Ludwig and T.B. Clegg, Phys. Rep. **201**, 57(1991).
- [4] B.A. Watson, P.P. Singh and R.E. Segel, Phys. Rev. **182**, 977(1969).
- [5] F.D. Becchetti, Jr. and G.W. Greenlees, Phys. Rev. **182**, 1190(1969).
- [6] A. Nadasen, P. Schwandt, P.P. Singh, W.W. Jacobs, A.D. Bacher, P.T. Debevec, M.D. Kaithuck and J.T. Meek, Phys. Rev. **C23**, 1023(1981).
- [7] P. Schwandt, H.O. Meyer, W.W. Jacobs, A.D. Bacher, S.E. Vigdor, M.D. Kaithuck and T.R. Denoghue, Phys. Rev. **C26**, 55(1982).
- [8] R.L. Walter and P.P. Guss, Proc. Int. Conf. on Nuclear Data for Basic and Applied Sciences, Santa Fe, N.M., U.S.A. Gordon and Breach, p.1079(1986).
- [9] J.H. Dave and C.R. Gould, Phys. Rev. **C28**, 2212(1983).
- [10] J. Rapaport, V. Kulkarni and R.W. Finlay, Nucl. Phys. **A330**, 15(1979).
- [11] E.D. Cooper, B.C. Clark, R. Kozak, S. Shim, S. Hama, J.I. Johansson, H.S. Scherif, R.L. Mercer and B.D. Serot, Phys. Rev. **C36**, 2170(1987).
- [12] S. Hama, B.C. Clark, E.D. Cooper, H.S. Scherif and R.L. Mercer, Phys. Rev. **C41**, 2737(1990).
- [13] R. Kozack and D.G. Madland, Nucl. Phys. **A509**, 664(1990).
- [14] F. Perey and B. Buck, Nucl. Phys. **32**, 79(1962).
- [15] D. Wilmore and P.E. Hodgson, Nucl. Phys. **55**, 673(1964).
- [16] B.C. Clark, S. Hama, R.L. Mercer, L. Ray, G.W. Hoffmann, and B. Serot, Phys. Rev. **C28**, 1421(1983).
- [17] J.-P. Jeukenne, A. Lejeune and C. Mahaux, Phys. Rev. **C 16**, 80(1977).
- [18] F.A. Brieva and J.R. Rock, Nucl. Phys. **A291**, 317(1977).
- [19] N. Yamaguchi, S. Nagata and T. Matsuda, Prog. Theor. Phys. **70**, 459(1983).
- [20] A.M. Lane, Nucl. Phys. **35**, 676(1962).
- [21] B.C. Clark, S. Hama, E. Sugarbaker, M.A. Franey, R.L. Mercer, L. Ray, G.W. Hoffmann and B.D. Serot, Phys. Rev. **C30**, 314(1984).
- [22] I. Tanihata, T. Kobayashi, T. Suzuki, K. Yoshida, S. Shimoura, K. Sugimoto, K. Matsuta, T. Minamisono, W. Christie, D., Olson and H. Wieman, Phys. Lett. **B287**, 307(1992).
- [23] J. Aichelin, G. Peilert, A. Bohnet, A. Rosenhauser, H. Stöcker. and W. Greiner, Phys. Rev. **C37**, 2451(1988).
- [24] G. Peilert, J. Konopka, H. Stöcker, W. Greiner, M. Blann and M.G. Mustafa, Phys. Rev. **C46**, 1457(1992).
- [25] T. Maruyama, A. Ohnishi and H. Horiuchi, Phys. Rev. **C45**, 2355(1992).
- [26] K. Niita, S. Chiba, T. Maruyama, T. Maruyama, H. Takada, T. Fukahori, Y. Nakahara, and A. Iwamoto, Phys. Rev. **C52**, 2620(1995).
- [27] M.B. Chadwick, S. Chiba, K. Niita, T. Maruyama and A. Iwamoto, Phys. Rev. **C52**, 2800(1995),
- [28] S. Chiba, M.B. Chadwick, K. Niita, T. Maruyama, T. Maruyama and A. Iwamoto, Phys. Rev. **C53**, 1824(1996).

- [29] S. Chiba, O. Iwamoto, T. Fukahori, K. Niita, T. Maruyama, T. Maruyama and A. Iwamoto, Phys. Rev. C **54**, 285(1996).
- [30] S. Chiba, K. Niita and O. Iwamoto, Phys. Rev. C., Dec. 1996 (in press).
- [31] T. Maruyama, K. Niita, T. Maruyama, S. Chiba, Y. Nakahara, and A. Iwamoto, Prog. Theor. Phys. **96**, 263(1996).
- [32] T. Maruyama et al., to be submitted.
- [33] H. Sorge, H. Stöcker, and W. Greiner, Ann. of Phys. **192** (1989) 266
- [34] T. Maruyama, S. W. Huang, N. Ohtsuka, G. Q. Li, A. Fässler, and J. Aichelin, Nucl. Phys. A **534** (1991) 720
- [35] T.H.R. Skyrme, Nucl. Phys. **9**, 615(1959).
- [36] J. Cougnon, private communication.
- [37] W. Bauhoff, Atomic Data and Nuclear Data Tables, **35**, 429(1986).
- [38] A. Auce, R.F. Carlson, A.J. Cox, A. Ingemarsson, R. Johansson, P.U. Renberg, O. Sundberg and G. Tibell, Phys. Rev. C **53**, 2919(1996).
- [39] M. Nolte, H. Machner and J. Bojowald, Phys. Rev. C **36**, 1312(1987).
- [40] A. Ohnishi, *Microscopic Simulation of Nuclear Reaction as a Tool to Evaluate Nuclear Data*, NRDF Annual Report 93, Hokkaido University (1994) (in Japanese).
- [41] I. Tanihata, H. Hamagaki, O. Hashimoto, Y. Shida, N. Yoshikawa, K. Sugimoto, O. Yamakawa, T. Kobayashi and N. Takahashi, Phys. Rev. Lett. **55**, 2676(1985).
- [42] I. Tanihata, T. Kobayashi, O. Yamakawa, S. Shimoura, K. Ekuni, K. Sugimoto, N. Takahashi, T. Shimoda and H. Sato, Phys. Lett. **B206**, 592(1988).
- [43] H. Bethe, Phys. Rev. **57**, 1125(1940).
- [44] M.S. Hussein, R.A. Rego and C.A. Bertulani, Phys. Rep. **201**, 279(1991).
- [45] R. W. Finlay, *Precision Total Cross Sections and the Optical Model at Intermediate Energy*, Proc. Int. Symp. on Fast Neutron Physics, 9-13 Sept. 1991, Beijing, China, World Scientific, p.299(1992).